

Supporting Information for

Cooperation between subunits is essential for high affinity binding of *N*-acetyl-D-hexosamines to dimeric soluble and dimeric cellular forms of human CD69

Daniel Kavan,^{§,||} Monika Kubíčková,[‡] Jan Bílý,[§] Ondřej Vaněk,^{§,||} Kateřina Hofbauerová,^{||} Hynek Mrázek,^{§,||} Daniel Rozbeský,[§] Pavla Bojarová,^{§,||} Vladimír Křen,^{||} Lukáš Žídek,[‡] Vladimír Sklenář,[‡] and Karel Bezouška,^{||,§}

[§]*Department of Biochemistry, Faculty of Science, Charles University, 12840 Prague, Czech Republic,* ^{||}*Institute of Microbiology, Academy of Sciences of Czech Republic, 14220 Prague, Czech Republic,* [‡]*National Centre for Biomolecular Research, Faculty of Science, Masaryk University, 61137 Brno, Czech Republic*

Supporting Methods.

Binding of calcium to soluble CD69 proteins. Binding of calcium to soluble CD69 protein was performed using $^{45}\text{CaCl}_2$ (Perkin Elmer) diluted to the desired specific radioactivity with the unlabeled calcium chloride essentially as described previously (17). Briefly, defined concentrations of individual soluble CD69 proteins in MES + C buffer pH 6.0 (10 mM MES with 0.15 M NaCl, 1 mM CaCl_2 , and 1mM NaN_3) were placed in 200 μl into a protein compartment, while the diluted radiolabeled ligands were placed in 200 μl into the ligand compartment. The two compartments were separated by a Spectra Pore tubing with 3000 molecular weight cutoff. Both compartments were rotated at 50 rpm at 30 °C for 24 h to establish the equilibrium. Thereafter, 20 μl samples were withdrawn from both compartments for the determination of radioactivity by liquid scintillation counting (^{45}Ca has a spectrum similar to ^{33}P that was used without any correction). The binding data were evaluated using a Scatchard plot according to the protocol implemented by Rosenthal as described previously (S1). For plots with one class of binding sites, the intercept on the abscissa gives the number of binding sites per mole of CD69 subunits, and the slope gives $-1/K_d$, where K_d is the dissociation constant for the interaction of the ligand with the protein.

Plate binding and plate inhibition assays. Inhibition assays were performed as described previously (17, S2), with the difference that the soluble CD69 proteins were labeled with florescent labels (fluorescein and rhodamine, respectively) using *N*-hydroxysuccinimide fluorescein and *N*-hydroxysuccinimide rhodamine (both from Pierce Biotechnology, USA, 25). The concentration of the bound protein receptors in the microtiter wells was determined by fluorescence ($\lambda_{\text{ex}}/\lambda_{\text{em}} = 496/519$ nm and $\lambda_{\text{ex}}/\lambda_{\text{em}} = 546/577$ nm, respectively) using Safire 2 spectrophotometer (Tecan, Austria). The results are given as a negative logarithm of the ligand concentration required to cause 50 % inhibition of binding of the receptor to the standard high affinity ligand $\text{GlcNAc}_{17}\text{BSA}$ ($-\log \text{IC}_{50}$).

Supporting References

- S1. Rosenthal, H. E. (1967) A graphic method for the determination and presentation of binding parameters in a complex system. *Anal. Biochem.* 20, 525-532.
- S2. Bezouška, K., Vlahas, G., Horváth, O., Jinochová, G., Fišerová, A., Giorda, R., Chambers, W. H., Feizi, T., and Pospíšil M. (1994) Rat natural killer cell antigen, NKR-P1, related to C-type animal lectins is a carbohydrate-binding protein. *J. Biol. Chem.* 269, 16945-16952.

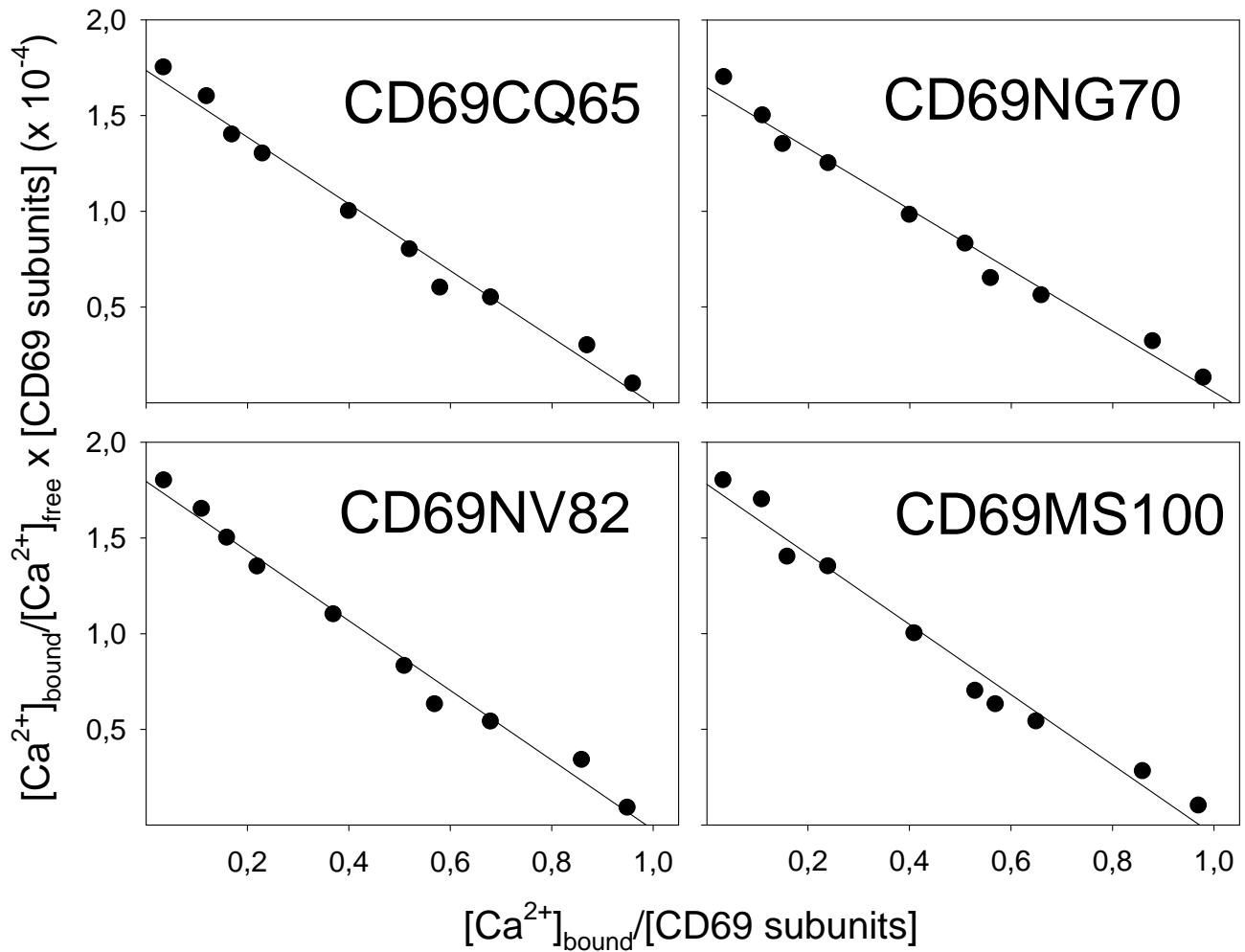
Supporting Table S1

Table 1. Summary of CD69 protein constructs used in the previous and current studies.

Construct ¹	Designation	Production method	Amino acids	Native protein	Method of verification ²	Reference
R1	CDA301	MBP fusion	Q65-K199	Dimeric	S, G	15
R2	rCD69	His tagged	Q65-K199	Dimeric	S, G, I, M	16
R3	CD69MS100	Direct expr.	S100-K199	Monomeric	S, G, I, M	17
R4	CD69CQ65	His tagged	Q65-K199	Dimeric	S, G, M	18
	CD69NG70	Direct expr.	G70-K199	Dimeric	S, G, M, N	18
	CD69NV84	Direct expr.	V82-K199	Dimeric	S, G, M, N	18
P	CD69Q93A	Direct expr.	G70-K199 ³	Dim/Mon	S, G, M, N	P
P	CD69R134A	Direct expr.	G70-K199 ³	Dim/Mon	S, G, M, N	P
P	CD69QRDM	Direct expr.	G70-K199 ³	Mon	S, G, M, N	P
N/Ch	I-CD69WT	Transfection	M1-K199	Dimeric	S, I, F	8
N/Ch	IIA.	Transfection	Q38-K199 ⁴	Dimeric	S, I, F	8
N/Ch	IIB	Transfection	P77-K199 ⁴	Trimeric	S, I, F	8
N/Ch	IIIA	Transfection	M1-P77 ⁴	Dimeric	S, I, F	8
N/Ch	IIIB	Transfection	M1-G64 ⁴	Trimeric	S, I, F	8
N/M-P	Q	Transfection	M1-K199 ³	Dimeric	S, I, F	P
N/M-P	R	Transfection	M1-K199 ³	Dimeric	S, I, F	P
N/M-P	QR	Transfection	M1-K199 ³	Dimeric	S, I, F	P
N/M-P	C	Transfection	M1-K199 ³	Dimeric	S, I, F	P
N/M-P	CQ	Transfection	M1-K199 ³	Dimeric	S, I, F	P
N/M-P	CR	Transfection	M1-K199 ³	Dim/Mon	S, I, F	P
N/M-P	CRQ	Transfection	M1-K199 ³	Monomeric	S, I, F	P

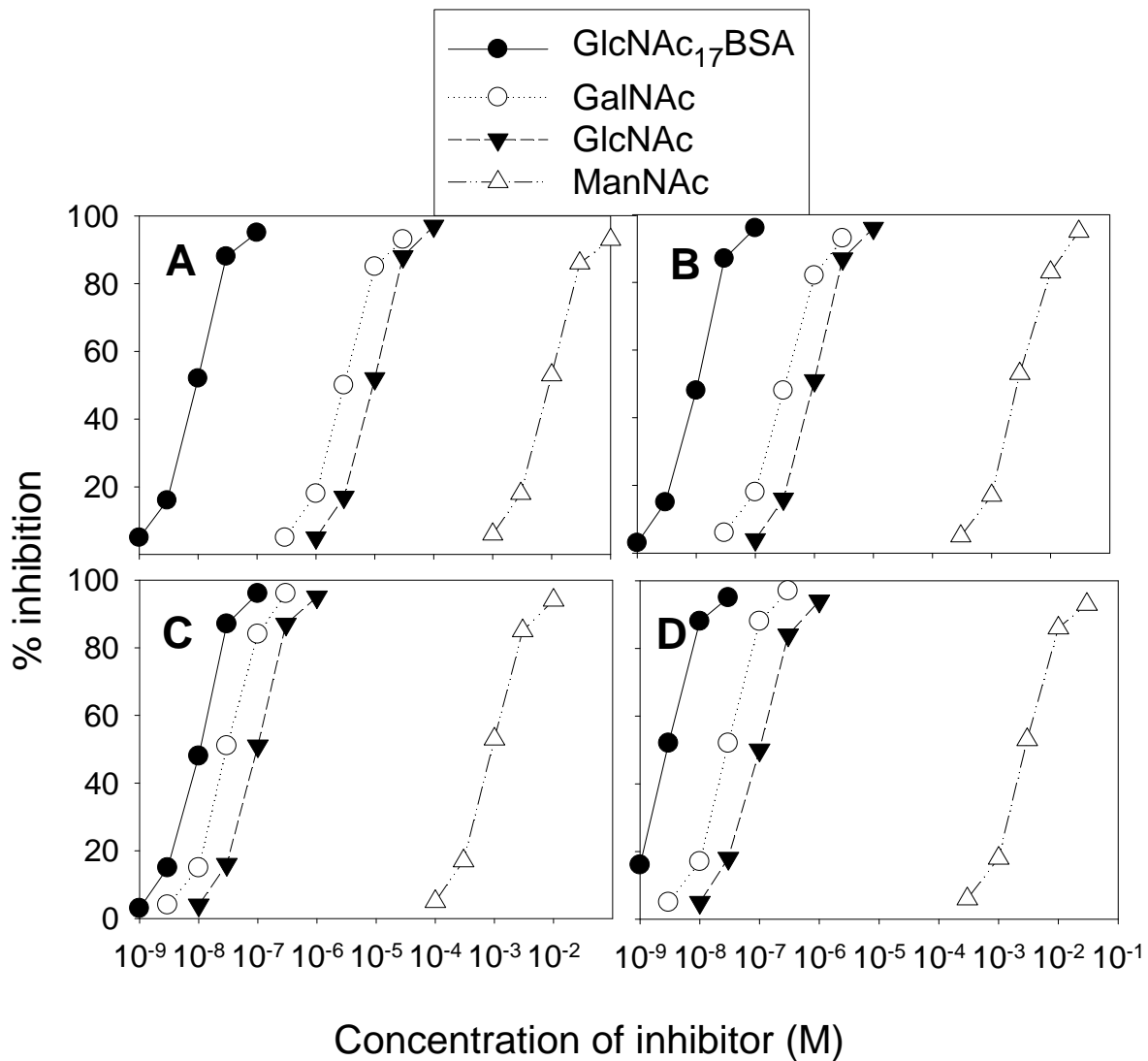
¹R, recombinant protein; P, present work; N/CH, native CD69/CD23 chimeric proteins; N/M-P, native mutated proteins in the present work. ²S, SDS-PAGE; G, gel filtration, I, immunochemical analysis, M, mass spectrometry, N, NMR, F, functional assay; ³Additional mutations are contained within the internal amino acid sequence of this protein; ⁴Fusion with portions of CD23 lymphocyte receptor.

Supporting Figure S1



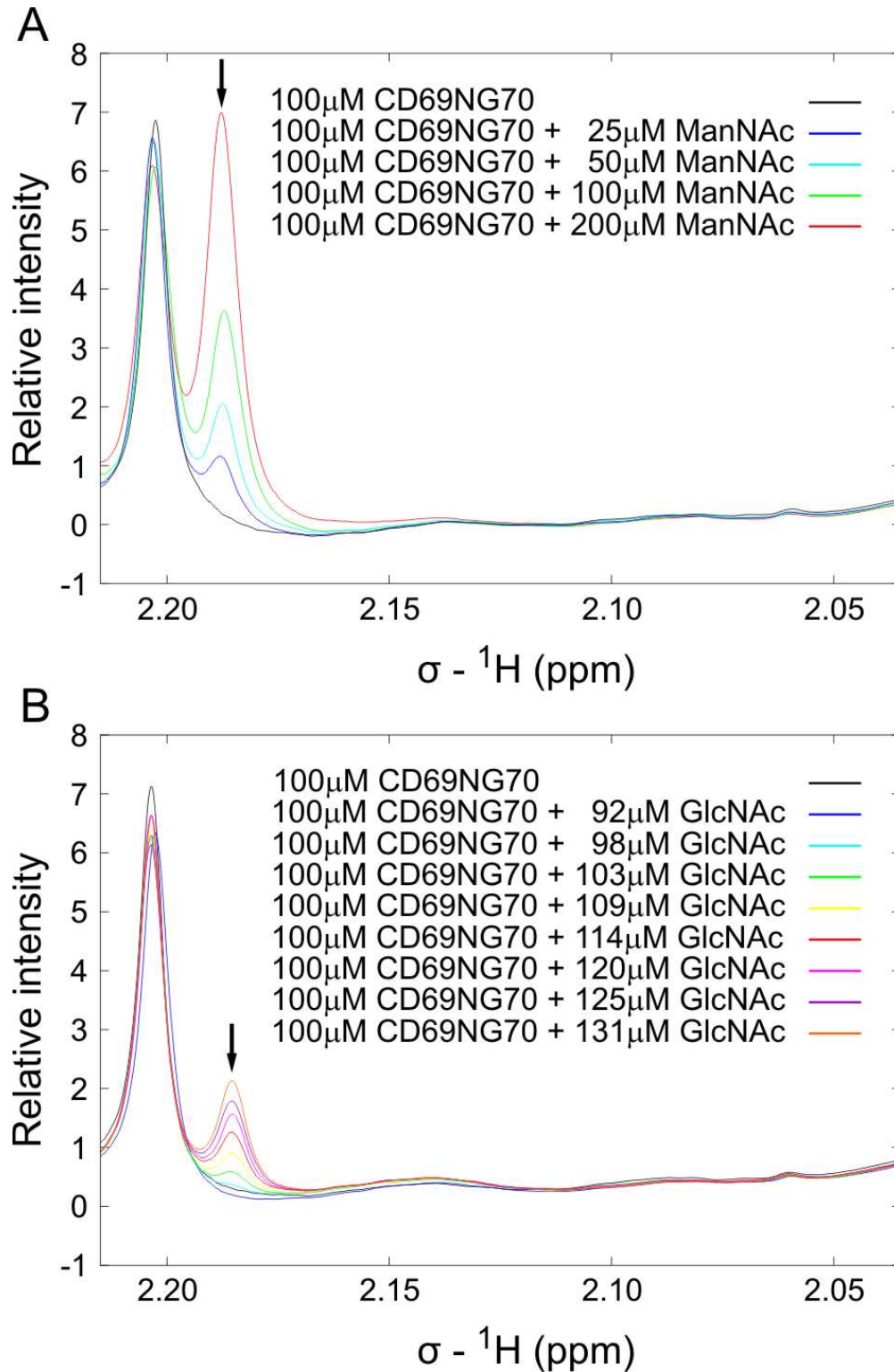
Supporting Figure S1. Binding of calcium to three soluble CD69 proteins based on the fourth generation constructs (CD69CQ65, CD69NG70, and CD69NV82, ref. 18) compared to soluble CD69 protein based on the third generation construct (CD69MS100, ref. 17). The binding of calcium to all four protein was essentially identical, with one mole of calcium being bound to one mole of CD69 subunits with K_d of approximately 50 μ M, the same as reported previously (17). For further details of the experiment, see the Supporting Methods.

Supporting Figure S2



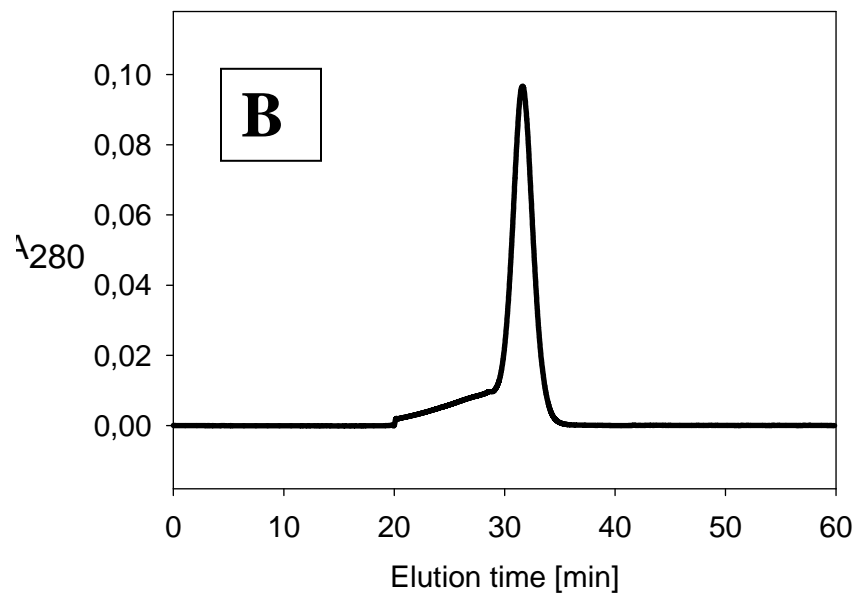
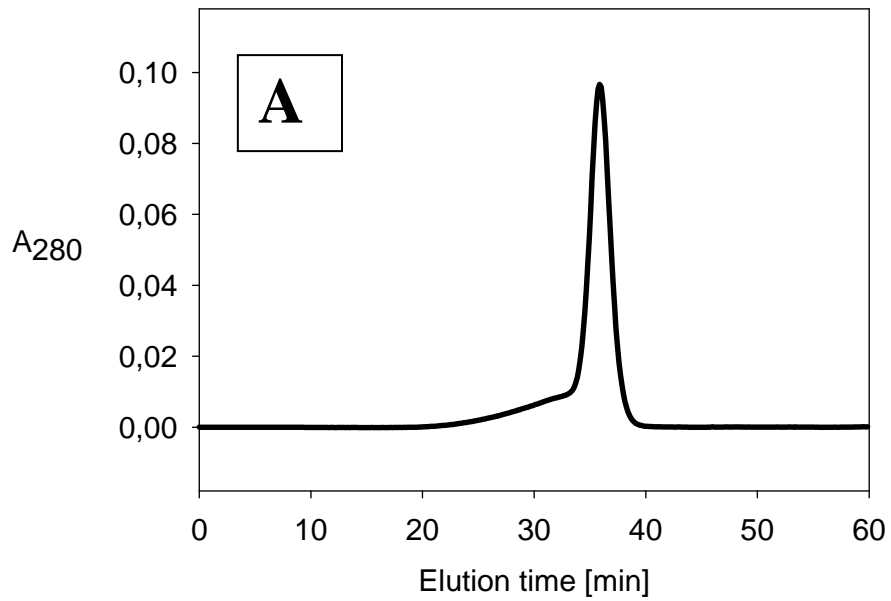
Supporting Figure S2. Inhibition of binding of soluble CD69 proteins to microtiter wells coated by the high-affinity ligand, GlcNAc₁₇BSA with neoglycoprotein and monosaccharide ligands. Microplate wells were coated overnight with GlcNAc₁₇BSA, washed, blocked with 2 % BSA, and used to measure inhibition of binding of the respective soluble CD69 proteins labeled by fluorescent labels to the immobilized high affinity ligand. The examined proteins were CD69MS100 (A), CD69NV82 (B), CD69NG70 (C), and CD69CQ65(D). For further details of the experiment, see Supporting Methods.

Supporting Figure S3



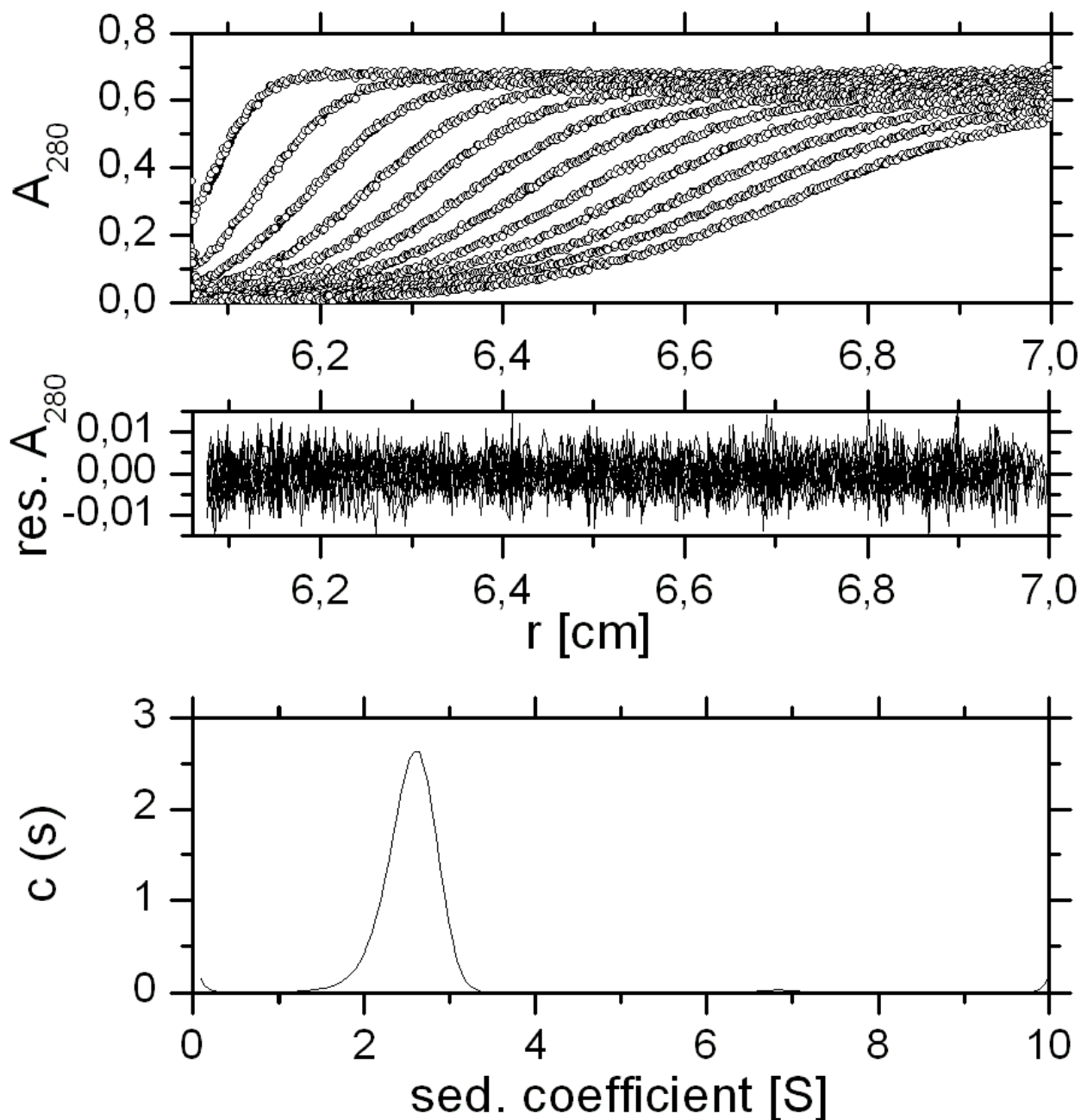
Supporting Figure S3. Overlaid one-dimensional proton NMR spectra taken in the course of titration of CD69NG70 with ManNAc (top) and GlcNAc (bottom). The displayed spectra were used to obtain concentrations of free *N*-acetyl-D-hexoseamines plotted in Fig. 2A and Fig. 2B, respectively.

Supporting Figure S4



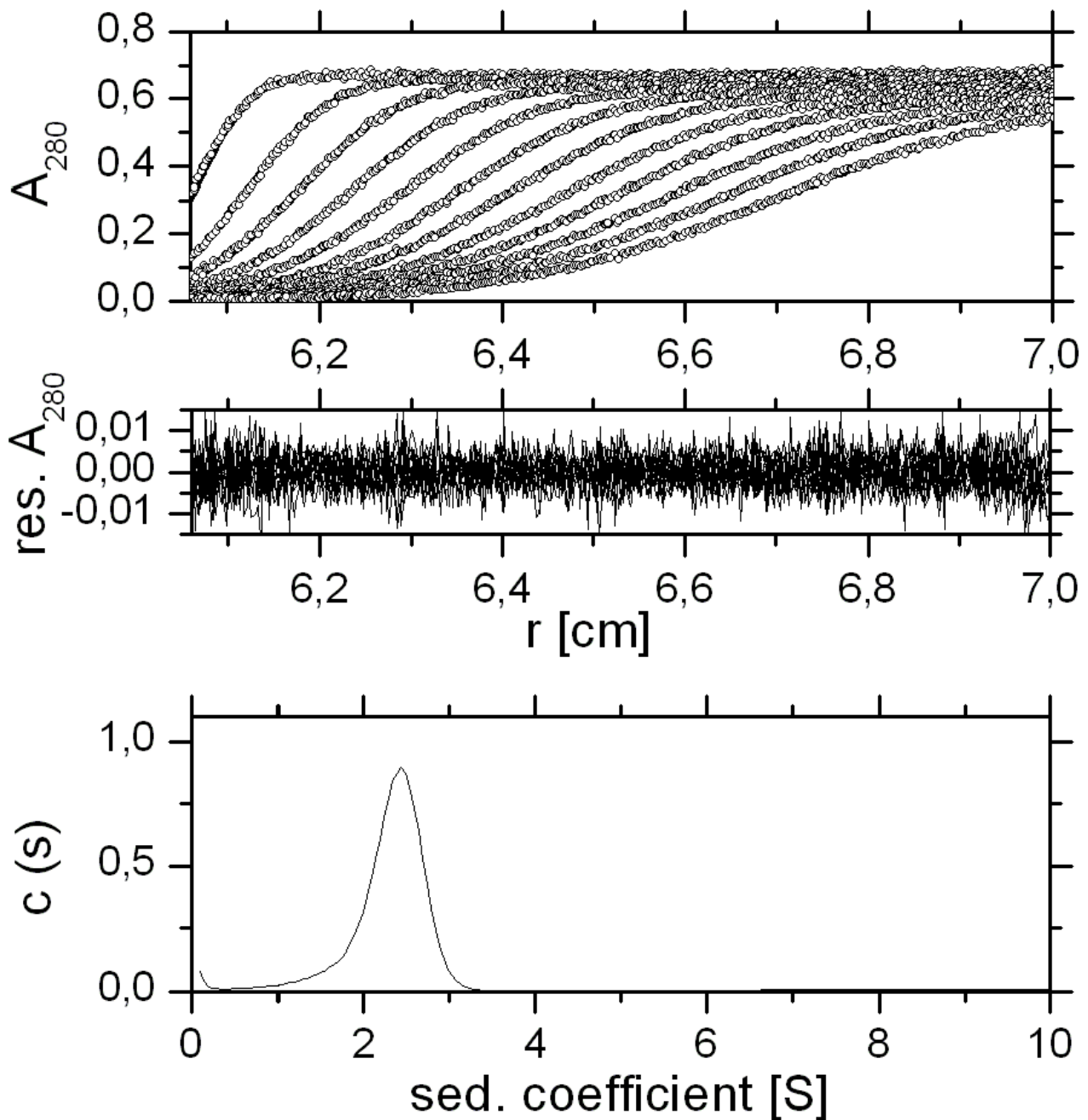
Supporting Figure S4. Changes in the hydrodynamic volume of soluble dimeric CD69 protein CD69NG70 in the presence of 1 mM ManNAc (A), and 1 mM GlcNAc (B), respectively.

Supporting Figure S5A



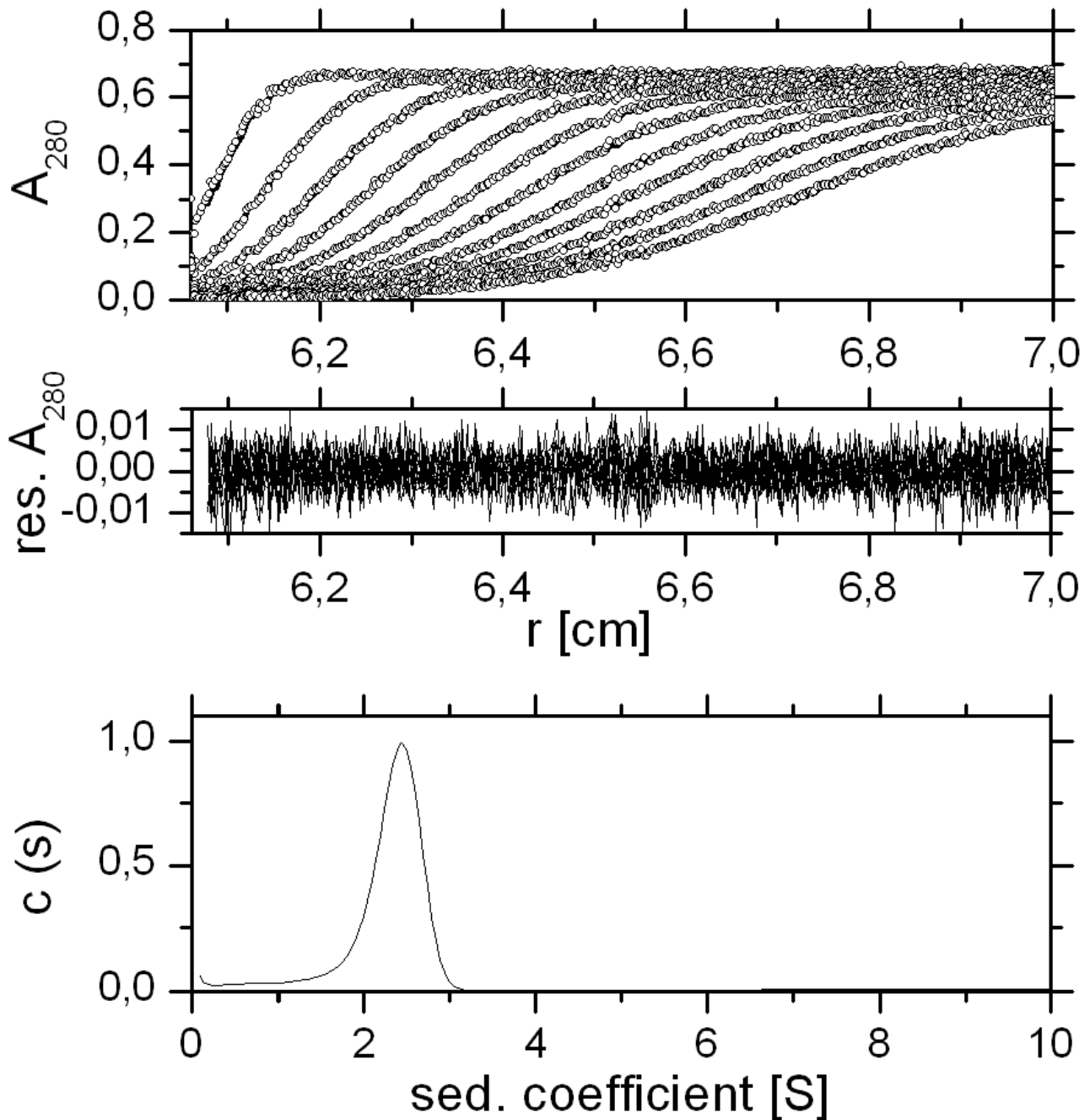
Supporting Figure S5A. Conformational change in recombinant soluble CD69 protein CD69NG70 shown by analytical ultracentrifugation analysis. The protein in the presence absence of any monosaccharide ligand (S4A), or in the presence of 1 mM ManNAc (S4B), or in the presence of 1 mM GlcNAc (S4C), respectively, was analyzed by sedimentation velocity. Panels show (from *top* to *bottom*) absorbance scans recorded each 5 min at rotor speed 48000 rpm (only every fifth scan is displayed), residuals derived from the fitted data, and distribution of the sedimentation coefficient derived using software SEDFIT.

Supporting Figure S5B



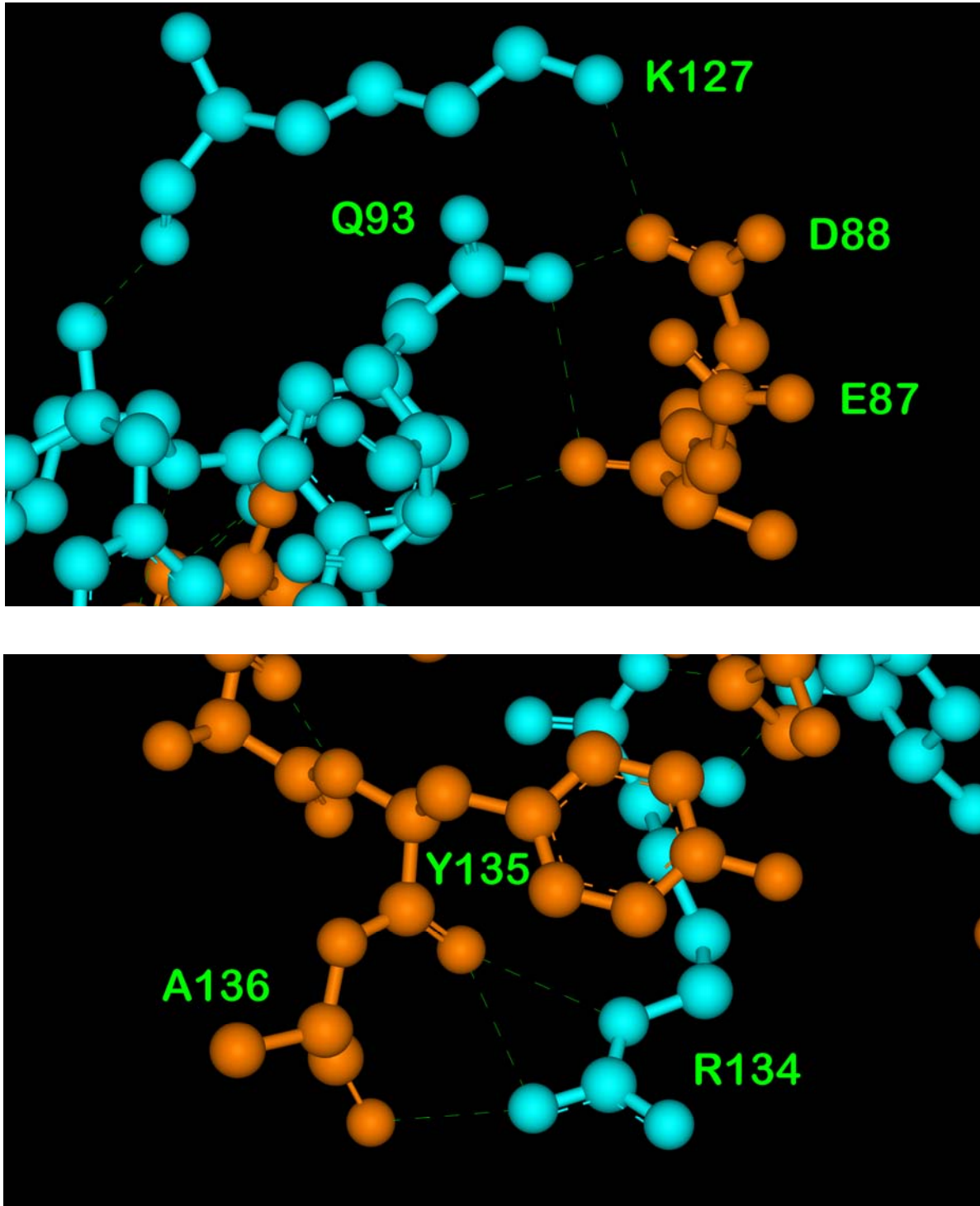
Supporting Figure S5B. Conformational change in recombinant soluble CD69 protein CD69NG70 shown by analytical ultracentrifugation analysis. The protein in the presence absence of any monosaccharide ligand (S4A), or in the presence of 1 mM ManNAc (S4B), or in the presence of 1 mM GlcNAc (S4C), respectively, was analyzed by sedimentation velocity. Panels show (from *top* to *bottom*) absorbance scans recorded each 5 min at rotor speed 48000 rpm (only every fifth scan is displayed), residuals derived from the fitted data, and distribution of the sedimentation coefficient derived using software SEDFIT.

Supporting Figure S5C



Supporting Figure S5C. Conformational change in recombinant soluble CD69 protein CD69NG70 shown by analytical ultracentrifugation analysis. The protein in the presence absence of any monosaccharide ligand (S4A), or in the presence of 1 mM ManNAc (S4B), or in the presence of 1 mM GlcNAc (S4C), respectively, was analyzed by sedimentation velocity. Panels show (from *top to bottom*) absorbance scans recorded each 5 min at rotor speed 48000 rpm (only every fifth scan is displayed), residuals derived from the fitted data, and distribution of the sedimentation coefficient derived using software SEDFIT.

Supporting Figure S6



Supporting Figure S6. Analysis of the dimer interface in CD69. (A) Interaction between Q93, K127, D88 and E87 at the dimer interface. (B) Interaction of R134, Y135, and A136 at the dimer interface. The residues from different subunits of CD69 are shown in cyan and orange; hydrogen bonds connecting highlighted residues are shown as broken green lines.